

Axial-Flux Synchronous Machines Compared with Different Stator Structures for Use in Working

Abstract. In this study, three different stator topologies were investigated and compared utilizing 3D magnetic analysis, analytical calculations, and experimental studies. These stator structures are torus iron core. There have been far fewer studies based on slotless stator torus axial-flux permanent magnets (TAFPM-NS). Comparisons of simulated and measured values on prototype machines are also presented to validate the analyses.

Streszczenie. W artykule przedstawiono wyniki prac dotyczących bezźłobkowego torusa stojana maszyny synchronicznej z magnesami trwałymi o strumieniu osiowym (ang. torus axial-flux permanent machine – TAFPM-NS). Materiał przedstawia badania i porównanie trzech typów stojana, na podstawie analizy magnetycznej 3-D oraz fazy eksperymentalnej. (Porównanie struktur stojana maszyny synchronicznej o strumieniu osiowym)

Keywords: Torus axial flux permanent magnet machines (TAFPM), finite element analysis (FEA), electric generators

Słowa kluczowe: Maszyna z magnesami trwałymi o osiowym strumieniu torusa (TAFPM), Metoda Elementów Skończonych (MES), generatory energii

1. Introduction

Axial-flux permanent magnet (AFPM) machines have become an important subject of study because of the development of neodymium magnets over the past 20 years. Axial-flux machines have high power density and high torque. Therefore, AFPM machines are in use in many areas. The literature contains many researches on AFPM machines, including some important studies on torus axial-flux permanent magnet (TAFPM) machines. The researches on TAFPM machines examine both types: slotted torus axial flux permanent magnet (TAFPM-S) machines, and non-slotted torus axial-flux permanent magnet (TAFPM-NS) machines. TAFPM-S type machines, however, have been the most frequently studied issue.

The most important properties of the TAFPM-S machines are their high power density and high torque. Their disadvantages include high cogging and ripple torque. Therefore, studies on the TAFPM-S machines have focused largely on the cogging and ripple torque. TAFPM-NS machines have great potential in many applications, due to their low manufacturing cost and zero cogging torque. TAFPM machines with coreless stators are used in electrical vehicles and generator applications.

In 1996, Caricchi and colleagues designed a multistage axial-flux permanent magnet machine. The first designs of AFPM machines featured coreless stators. Since AFPM machines use rhomboidal windings, the electromotive force (EMF) is nearly sinusoidal. The number of turns per coil is 9, and at 150 Hz, voltage $V_m=127$ is obtained [1]. In 2001, Aydin and colleagues presented 3D magnetic analyses of slotted and non-slotted torus-type axial-flux permanent magnet machines, investigating the effects that skewing the magnets had on performance of AFPM machines.

Lambda (λ) and air gap are the critical values in the optimization of AFPM machines [2, 3]. In 2005, Crescimbin and colleagues designed the slotted axial-flux permanent magnet generator for hybrid vehicle applications. In the design, the number of turns per coil was four. At 600 Hz, the authors obtained 90 volt rms (V_e). The design was water-cooled, and the windings current was 55.6 amperes. As can be seen in this study, the water-cooled design of the machines has a significant effect on power density [4].

In 2007, Rahim and colleagues designed the slotless axial flux permanent magnet machines (AFPM-NS). They used 3D magnetic analyses in the design of AFPM-NS. At 100 Hz, the authors obtained $V_m=150$ volts. The number of turns per coil was 21, and the rotor was composed of

trapezoidal magnets. Also in this study, the optimization of AFPM-NS machines was performing using various parameters such as air gap, permanent magnet, and winding dimensions [5]. In 2011, Mahmoudi and colleagues presented comparisons between slotted axial-flux one-stator, two-rotor (TAFPM) machines and two-stator, one-rotor (AFIR) machines by means of 3D magnetic analyses. As a result of the magnetic analysis, the power density of TAFPM machines is high relative to AFIR machines. AFPM-NS machines have negligible cogging torque, and ripple torque is also less [6].

In the literature, studies about non-slotted torus axial-flux permanent magnet (TAFPM-NS) machines are very few, and half of the studies are based solely on magnetic analysis. A review of experimental studies shows that the number of turns per coil for non-slotted AFPM machines is less than other machines. Thus, TAFPM-NS machines have lower power density than their slotted counterparts (TAFPM-S). In many studies, these machines have exhibited negligible cogging torque and lower ripple torque, which are key advantages. Employing external cooling techniques to increase the power density can improve performance of TAFPM-NS machines.

In this study, the stator windings of TAFPM-NS machines are composed of multilayer windings (MLW). TAFPM-NS machines with multilayer windings (MLW) have been compared to TAFPM-NS with one-layer windings and TAFPM-S machines to prove superiority. This paper shows that multilayer windings provide higher power density and easier stator construction than one-layer windings. Hence, the stator with multilayer windings can most readily improve the parameters of the TAFPM machines. Experimental studies comparing 3D magnetic and analytical studies has proved the accuracy of the results.

2. The Parameters of the Three Machines

The three different stator structures are pictured below. Figure 1 (a), (b), and (c), respectively, show the multilayer windings, one-layer windings, and slotted windings. The windings are three-phase, and the number of slots per pole per phase is $c=1$.

The identical and non-identical parameters of the three different stators are shown in Table 1.



Fig. 1. (a) Left: Stator with multilayer windings (MLW); (b) Center: Stator with one-layer windings; (c) Right: Stator with slotted torus.

Table 1. Electrical and mechanical parameters of the axial-flux machines

Identical parameters of the three different TAFPM machines			
Parameters of the rotor			
Magnet	NdFeB	Thickness of magnet	10mm
Remanance (Bc)	1.23 Tesla	External diameter	210mm
Coercivity (Hc)	890000 A/m	Internal diameter	130mm
BHmax	273.675	Rotor thickness	5mm
Pole number	14		
Parameters of the stator			
Coil type	Toroidal	Coil number per phase	14
Wire diameter	1mm	Iron core thickness	30mm
Iron core diameter	210mm	Type of iron core	MOH
Electrical features			
Rated current	10 A	Rated speed(rpm)	428 rpm
Non-identical parameters of the three different TAFPM machines			
	Three-layer windings	One-layer windings	Slotted stator windings
Number of turns per phase	18*14=252	7*14=98	17*14=252
Distance between iron core and magnets	6mm	3mm	2mm

The specifications in Table 1 describe the three different stators. Figure 1(a) shows a stator composed of multilayer windings (MLW) on an iron core. In the design, the air gap and the number of turns have been increased. The negative impact on electromotive force (EMF) of the increasing air gap has been reduced by increasing the number of turns; this situation is presented experimentally and analytically in Table 4. Figure 1(b) shows a stator composed of one-layer windings on an iron core. The air gap flux density of these machines is high, while the number of turns is low. Figure 1(c) shows the open slot axial flux machine composed of slotted stators. The air gap flux density of these machines is high, and the number of turns is also high. However, the biggest disadvantage is high values in cogging torque. These three stators have been investigated in the experimental mechanism shown in Figure 2. The experimental results are compared with magnetic and analytical calculations.



Fig. 2. Experimental setup

3. 3D Magnetic Analyses

The 3D model in Figure 3 has been designed for magnetic analyses of the three different stators. The most important value in the 3D model is the air gap magnetic flux density. Therefore, magnetic analysis between magnets and the iron core is enough to represent the different structures of stator. Along the line in Figure 3, the magnetic flux density has been computed for the different air gap values.

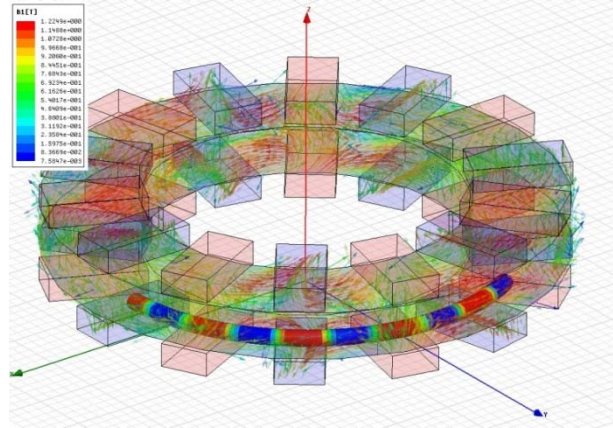


Fig. 3. Results of the magnetic analyses

Figure 4 shows magnetic flux densities calculated for various sizes of air gap ranging from 1mm to 10mm. The average magnetic flux density decreased with increases in the air gap values. This caused the induced voltage to decrease.

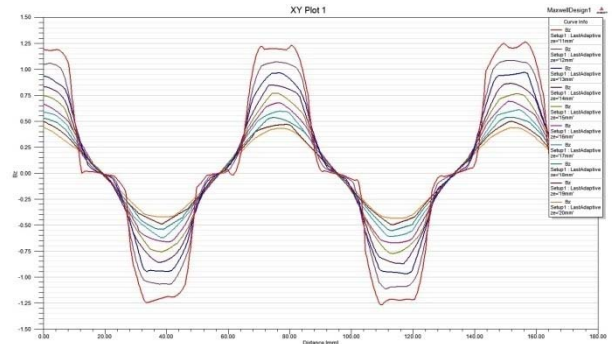


Fig. 4. Flux density contour (1mm – 10mm)

The values obtained from the 3D finite element analyses (FEA) are shown in Table 2. The air gap ranged from 1mm to 10mm. Values for Bavg, Bmax, and Bmin have been calculated for each size of air gap. The values of Bavg, Bmax, Bmin were found to decrease with increases in the air gap values.

Table 2. Magnetic flux values associated with air gaps of varying sizes

Air Gap	Bavg	Bmax	Bmin
1mm	1.066	1.229	0.246
2mm	0.929	1.072	0.290
3mm	0.815	0.969	0.361
4mm	0.714	0.850	0.335
5mm	0.628	0.772	0.320
6mm	0.559	0.679	0.285
7mm	0.501	0.597	0.274
8mm	0.451	0.538	0.256
9mm	0.400	0.470	0.216
10mm	0.369	0.434	0.211

In the literature, the maximum magnetic flux density of the high power density machine exceeds 0.6 tesla [8]. However, different studies have shown that AFPM

machines are designed with 0.55 tesla, 0.462 tesla, and 0.282 tesla values of the magnetic flux density [9 10 11]. Thus, from magnetic analyses, it is shown that the air gap of the AFPM machines should be 7mm or less.

4. Theoretical Analysis

Per phase induced voltages are calculated using equations obtained by the values of the magnetic flux density calculations.

The surface area of the iron core is calculated from formula 1.

$$(1) \quad S = \pi(r_1^2 - r_2^2) \text{ (cm}^2\text{)}$$

$$(2) \quad Q = \frac{BS}{2P} \text{ (weber)}$$

$$(3) \quad E_f = 4.44 * Q * f * N_f * K_w \text{ (Volt)}$$

$$(4) \quad E_m = 1.44 * E_f$$

Table 3 presents the calculated values from both simulation results and the above formulas. The point to be considered in the calculations is that simulation results were obtained from a one sided-stator, so E_m and E_f are divided by 2.

Table 3. The induced voltage values of different air gaps

Air Gap (mm)	B (Tesla)	$E_f/2$ (Volt)	$E_m/2$ (Volt)
1	1.10	46.92	67.57
2	0.97	41.38	59.58
3	0.86	36.68	52.83
4	0.79	33.70	48.53
5	0.70	29.86	43.00
6	0.64	27.30	39.31
7	0.56	23.89	34.40
8	0.51	21.75	31.33
9	0.45	19.19	27.64
10	0.40	17.06	24.57

According to the values given in Table 3, the induced voltage decreased with increases in the air gap.

5. Experimental Results

The values of the induced voltage in the constant frequency for three different stator structures are given in Figure 5. E_m produced by MLW, E_m produced by one-layer windings, and E_m produced by slotted stators, respectively, were 39.3V, 18.01V, and 49.4V. The induced voltages per turn, from largest to smallest, respectively, were slotted stators, the one-layer windings, and the multilayer windings. However, the number of turns of the one-layer windings is fewer than multilayer windings, because of the physical bounding, and in spite of the high values of the voltage/the number of turns for the one-layer windings. For the same current value, the power increased by 50 percent.

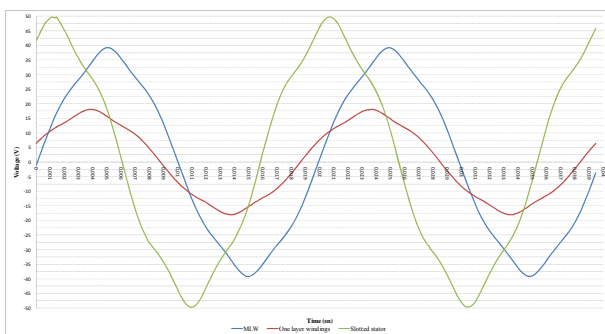


Fig. 5. Empty operating voltages

Figure 6 shows the voltage regulation for the different stator structures. The equal values of the current/the number of turns calculating voltage regulation were taken. The regulation of voltage from smallest to largest, respectively, were obtained for the slotted stator ($V_m=49.7-42.6=7.1$ V), the multilayer windings ($V_m=39.3-30.6=8.7$ V), and the one-layer windings ($V_m=18.1-7.42=10.68$ V).

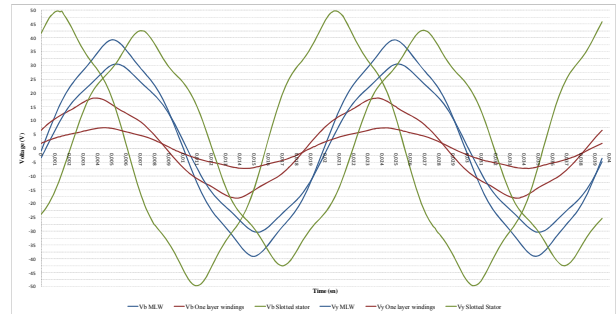


Fig. 6. The regulation of voltage

Table 4 compares the experimental results with analytical values calculated by the 3D FEA. The air gap in the slotted stator to reduce cogging torque is taken to be 3 mm. The experimental results for using one rotor showed the same values (i.e., they were not divided by 2).

Table 4. Comparing both analytical results via 3D FEA and experimental results

	Analytical results via 3D FEA			Experimental results E_m (Volt)
	B (Tesla)	$E_f/2$ (Volt)	$E_m/2$ (Volt)	
Multilayer windings	0.64	27.30	39.31	39.3
Slotted stators	0.86	36.68	52.83	49.7
One-layer windings	0.86	14.26	20.54	18.1

6. Conclusion

This study has investigated three different stator structures—multilayer windings, one-layer windings and slotted stators—and obtained analytical results and experimental results for empty work and loaded work. The magnetic and analytical calculations have been proven with experimental results, as shown in Table 4. Here are some of the findings:

- Due to the high number of turns, the MLW provide higher voltage and less voltage regulation than one-layer windings.
- The number of turns are the same for both slotted stators and MLW, so the slotted stator produces higher voltage than MLW.
- The voltage regulation in the slotted stator is lower than in the one-layer windings, and slotted stators have high cogging torque, while MLW stators do not have cogging torque. This situation in cogging torque is the biggest advantage of MLW stators.
- One-layer windings produce a lower voltage than slotted stators; hence the voltage regulation of the one-layer windings is higher than that of the slotted stator. The most important reason for this is that the number of turns is mechanically restricted by the stator surface. Therefore, the number of turns of the one-layer windings is much lower than slotted stators and MLW.
- The air gap magnetic flux density of the MLW is less. This situation is eliminated by the high number of turns.

- As seen from experimental study, the voltage of the MLW is high. Thus the stator of the MLW can easily be used in high-power applications.
- Due to their lack of cogging torque, MLW are preferred over slotted systems.

•

Acknowledgements

This work was supported by the commission on scientific research projects of Marmara University under Grant FEN-C-DRP-181208-0292.

REFERENCES

- [1] Caricchi F., Crescimbin F., Mezzetti F., Santini E., Multistage Axial Flux PM Machine for Wheel Direct Drive, *IEEE Transactions on Industry Applications*, July/August, (1996), Vol.32, No.4, 882-888
- [2] Huang S., Luo J., Leonardi F., Lipo T.A., A Comparison of Power Density for Axial Flux Machines Based on General Purpose Sizing Equations, *IEEE Transactions on Energy Conversion*, (1999), Vol.14, No.2, 185-192
- [3] Aydın M., Huang S., Lipo T.A., Design and 3D Electromagnetic Field Analysis of Non-slotted and Slotted Torus Type Axial Flux Surface Mounted Permanent Magnet Disc Machines, *IEEE Transactions on Energy Conversion*, (2001)
- [4] Crescimbin F., Di Napoli A., Solero L., Caricchi F., Compact Permanent-Magnet Generator for Hybrid Vehicle Applications, *IEEE Transactions on Industry Applications*, September/October, (2005), Vol.41, No.5, 1168-1177
- [5] Rahim N.A., Ping H.W., Tadjuddin M., Design of Axial Flux Permanent Magnet Brushless DC Motor for Direct Drive of Electric Vehicle, *IEEE Power Engineering Society General Meeting*, June, (2007)
- [6] Mahmoudi A., Ping H.W., Rahim N.A., A Comparison Between the Torus and AFIR Axial-Flux Permanent-Magnet Machine Using Finite Element Analysis, *IEEE International Electric Machines & Drives Conference (IEMDC)*, (2011), 242-247
- [7] Akuner C., Huner E., The Air Gap and Angle Optimization in the Axial Flux Permanent Magnet Motor, *Electronics and Electrical Engineering- Kaunas: Technologija*, (2011), No.4, 25-29
- [8] Gieras J.F., Gieras I.A., Performance Analysis of a Coreless Permanent Magnet Brushless Motor, *IEEE Industry Applications Conference*, (2002), Vol.4, 2477-2482
- [9] Marignetti F., Colli V.D., Cancelliere F., Scarano M., Boldea I., Topor M., A Fractional Slot Axial Flux PM Direct Drive, *IEEE*, (2008), 689-695
- [10] Sadeghierad M., Lesani H., Mosef H., Darabi A., Air Gap Optimization of High-Speed Axial Flux PM Generator, *Journal of Applied Sciences*, (2009), 1915-1921
- [11] Upadhyay P.R., Rajagopal K.R., Singh B.P., Design of a Compact Winding for an Axial Flux Permanent Magnet Brushless DC Motor Used in an Electric Two Wheeler, *IEEE Transactions on Magnetics*, July, (2004), Vol.40, No.4, 2026-2028

Authors: Engin Hüner, Marmara University, Department of Technical Education Faculty, Istanbul, Turkey, E-mail: engin.huner@marmara.edu.tr; dr Caner Akuner, Marmara University, Department of Technical Education Faculty, Istanbul, Turkey, E-mail: akuner@marmara.edu.tr